

Infrared spectroelectrochemistry of $[\text{Co}_3(\text{CPh})(\text{CO})_9]$ in methanol at a platinum electrode

Paula A. Brooksby, Noel W. Duffy, A. James McQuillan,^{*†} Brian H. Robinson and Jim Simpson

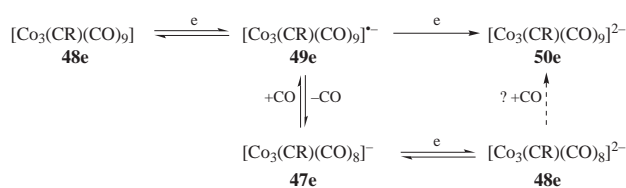
Department of Chemistry, University of Otago, PO Box 56, Dunedin, New Zealand

In situ infrared spectroelectrochemistry [SNIFTIRS (subtractively normalized interfacial FTIR spectroscopy)] has been used to obtain spectra at a platinum electrode of the reduction products of $[\text{Co}_3(\text{CPh})(\text{CO})_9]$ in absolute methanol, in CO saturated methanol, in the presence of a ligand $[\text{P}(\text{C}_6\text{H}_4\text{SO}_3\text{-}m)_3]^{3-}$ (L) and in dichloromethane. The cluster species 49e $[\text{Co}_3(\text{CPh})(\text{CO})_9]^{-}$, 50e $[\text{Co}_3(\text{CPh})(\text{CO})_9]^{2-}$ and, tentatively, the 47e $[\text{Co}_3(\text{CPh})(\text{CO})_8]^{-}$ and 48e $[\text{Co}_3(\text{CPh})(\text{CO})_8\text{L}]^{-}$ were identified and their interrelationships elucidated. Adsorption of the cluster at the surface may be responsible for the unexpected formation of CO_2 upon decomposition of $\text{Co}(\text{CO})_4^{-}$.

Electron-transfer processes in metal–metal bonded clusters have been probed primarily using cyclic voltammetry.¹ Clusters with strong π -acceptor ligands, such as CO, normally undergo one-electron reduction to the radical anion as the primary process whereas clusters with donor ligands, such as cyclopentadienyl or phosphines, may be oxidised to the radical cation. Control of the redox chemistry is therefore possible by tuning the ligand sphere.² The most important consequence of radical anion or radical cation formation is activation of the cluster towards nucleophilic substitution. This has allowed a number of efficient electron-transfer catalysed (ETC) cycles to be devised^{2,3} with considerable synthetic utility.^{3,4}

One of the most studied family of systems is that based on the tricobaltcarbon cluster² $[\text{Co}_3(\text{CR})(\text{CO})_9]$. The electrochemical behaviour of these clusters and their phosphine derivatives has been examined^{5–7} in several non-aqueous solvents, MeCN, acetone, thf and CH_2Cl_2 . These clusters primarily undergo reversible reduction to the 49e radical anion, with the unpaired electron occupying an a_2 SOMO centred on the Co_3 framework,⁸ followed by the irreversible formation of a 50e dianion. This dianion rapidly undergoes Co–Co bond cleavage giving the electroactive species $\text{Co}(\text{CO})_4^{-}$. The activated 49e radical anion then participates in rapid ETC ligand exchange reactions, both within the electrode double layer and in bulk solution. It has been suggested⁷ that a key step in these reactions is the reversible loss of CO to give a co-ordinatively unsaturated 47e anion which can be further reduced to a 48e dianion (Scheme 1). The kinetic data could also be compatible with Co–Co edge cleavage as the rate determining step. Although the 49e radical anion has been isolated and characterised^{9,‡} there are features of Scheme 1 which are still puzzling. We have shown¹⁰ that the essential electrochemical processes are unchanged in water or aqueous methanol, including rapid ETC reactions. Electrochemical experiments with $[\text{Co}_3(\text{CR})(\text{CO})_9]$ clusters in non-aqueous solutions at platinum electrodes often show some data variability which appears to indicate adsorption of cluster material.

This work sets out to provide a spectroscopic test of the proposed mechanisms and to generate new molecular information about the reaction products. Methanol is similar to water in many respects but much more suitable for infrared studies with generally weaker infrared absorptions and a wider potential



Scheme 1

window. It has no large absorptions in the carbonyl region and thus provides a good medium to investigate the $[\text{Co}_3(\text{CR})(\text{CO})_9]$ cluster. The IR spectroelectrochemistry of absolute methanol solutions has been studied by Pham *et al.*¹¹ and Brooksby *et al.*¹² and the reduction and oxidation behaviour of absolute methanol is well documented. It was also of importance to investigate the cluster configuration at the electrode surface using spectroscopic methods which have proved successful in investigations with organic substrates.¹³

Results and Discussion

Cyclic voltammetry of $[\text{Co}_3(\text{CPh})(\text{CO})_9]$ in absolute methanol and CO saturated methanol

A cyclic voltammogram between +0.4 and –0.9 V of $1.0 \times 10^{-3} \text{ mol dm}^{-3}$ $[\text{Co}_3(\text{CPh})(\text{CO})_9]$ in absolute methanol containing 0.1 mol dm^{-3} NaClO_4 electrolyte is shown in Fig. 1(i). The negative potential limit is close to that for the onset of dianion formation.⁵ The primary redox process depicted by the waves at A and B is that associated with the 48e/49e couple $[\text{Co}_3(\text{CPh})(\text{CO})_9]^{0/-}$. Peak C is due⁵ to the oxidation of $\text{Co}(\text{CO})_4^{-}$, a decomposition product of a radical species.

When CO was present there was no voltammetric evidence for $\text{Co}(\text{CO})_4^{-}$ [Fig. 1(ii)]. This observation is similar to that of Hinkelmann *et al.*⁷ for $[\text{Co}_3(\text{CMe})(\text{CO})_9]$. Wave E is associated with methanol oxidation.

These results from methanol solutions are similar to the well documented results for $[\text{Co}_3(\text{CPh})(\text{CO})_9]$ and related clusters in aqueous¹⁰ and non-aqueous^{5,6} solvents. Extension of the potential range to –1.2 V for the cyclic voltammograms of $1.0 \times 10^{-3} \text{ mol dm}^{-3}$ $[\text{Co}_3(\text{CPh})(\text{CO})_9]$ in absolute methanol and in CO saturated methanol solutions showed little change [Fig. 1(iii),(iv)]. Reduction of $[\text{Co}_3(\text{CPh})(\text{CO})_9]^{-}$ to the 50e dianion is expected in this region but the –1.2 V potential limit is close to that for solvent decomposition. In Fig. 1(iii) an additional peak is observed at –0.94 V on the reverse scan which may arise from the oxidation of this dianion. This peak is again not observed when CO is present. Whether in solution or

[†] E-Mail: jmcquillan@alkali.otago.ac.nz

[‡] The green anion was prepared by sodium reduction of the cluster in thf and, after concentrating the solution, precipitated as the $\text{N}(\text{PPh}_3)_2^+$ salt. It was recrystallised from CH_2Cl_2 but no crystals suitable for X-ray diffraction work were obtained.

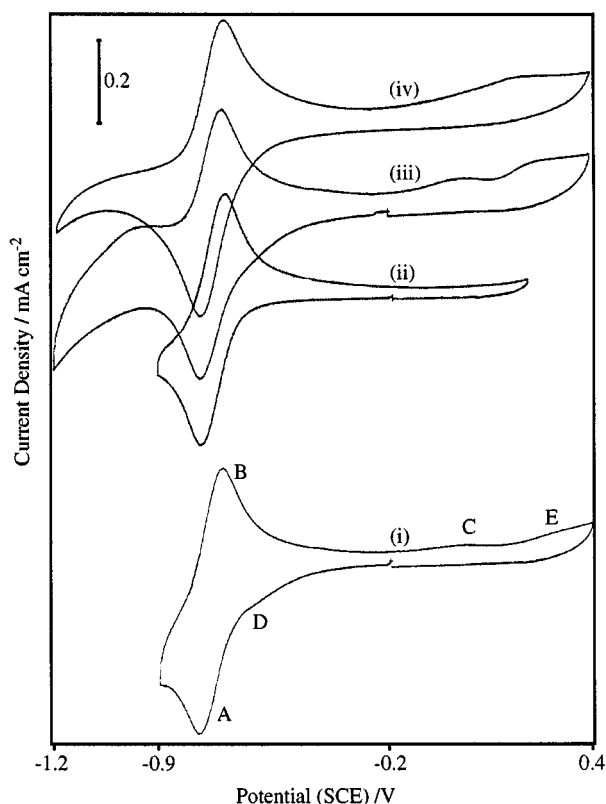


Fig. 1 Cyclic voltammograms of $1 \times 10^{-3} \text{ mol dm}^{-3} [\text{Co}_3(\text{CR})(\text{CO})_9]$ in methanol containing $0.1 \text{ mol dm}^{-3} \text{ NaClO}_4$ electrolyte. Scan rate = 100 mV s^{-1} . All scans were initially to more negative potentials from -0.2 V : (i) $+0.4$ to -0.9 V , N_2 saturated; (ii) $+0.2$ to -0.9 V , CO purged; (iii) $+0.4$ to -1.2 V , N_2 purged; (iv) $+0.4$ to -1.2 V , CO saturated

adsorbed on the surface CO plays a significant role in the electrochemistry.

The electrochemical behaviour of CO dissolved in methanol at a platinum electrode has been investigated.¹⁴ A featureless cyclic voltammogram within the solvent limits is observed between -1.0 and $+1.1 \text{ V}$ (vs. SCE). At the positive potential limit adsorbed CO is oxidised to CO_2 . At the negative potential limit adsorbed CO appears to desorb from the platinum surface. Carbon monoxide only affects the potential range where methanol oxidation and reduction occurs. The addition of $1.0 \times 10^{-3} \text{ mol dm}^{-3} [\text{Co}_3(\text{CPh})(\text{CO})_9]$ to a CO saturated methanol solution gave voltammetric waves for the primary couple unchanged from those already described [Fig. 1(ii)].

A small prepeak, **D**, appeared on all the initial scans where the platinum electrode was newly polished. This was not observed during the second or subsequent scans. It is not seen in aqueous solution,¹⁰ nor if the solution is purged with CO [Fig. 1(ii)]. The process which gives rise to **D** has been observed at intermittent times during scans conducted in acetone and dichloromethane, and is likely to be a feature that arises in low dielectric solvents. A prepeak, such as wave **D**, is generally^{15,16} associated with the strong adsorption of a reduction product, in this case the 49e radical anion. The absence of peak **D** during subsequent potential cycling, in methanol solutions without added CO , suggests that any adsorbed material remains on the platinum surface within the timescale of the voltammetry. Further adsorption of electroactive material is therefore blocked.

SNIFTIRS spectra of $[\text{Co}_3(\text{CPh})(\text{CO})_9]$ in CO saturated methanol

Infrared spectroscopic methods have been developing during the past two decades that allow the observation of molecular changes associated with electron transfer processes at elec-

trodes. Using the SNIFTIRS¹⁷ methodology, absorbance difference spectra that are induced by changes in potential are obtained. Species present at higher concentrations at the sampling potential (E_s) give rise to positive IR bands while those present at higher concentrations at the reference potential (E_r) give negative IR bands. The spectrum of the bulk solvent and electrolyte do not change with potential and are not observed. Ideal electrochemical cell behaviour is sacrificed in a SNIFTIRS thin layer cell and large solution resistances often result. The observation of species produced during reduction and oxidation reactions may therefore occur at potentials which are somewhat different to those observed during conventional electrochemical experiments.

Distinguishing between adsorbed and solution species is possible using the surface selection rules¹⁷ which predict differences between the spectra of adsorbed species for *s*- and *p*-polarised light. *p*-Polarised spectra contain information about both adsorbed and solution species while *s*-polarised spectra contain information about only solution species. A comparison of the spectra obtained using both types of polarisation will usually allow detection of adsorbed species, provided the absorptions arising from solution species do not obscure the generally weak absorptions of adsorbed species.

As shown in the voltammetry, CO saturated methanol solutions containing $[\text{Co}_3(\text{CPh})(\text{CO})_9]$ provide the least complex system to study and will be examined initially. An infrared solution spectrum of $[\text{Co}_3(\text{CPh})(\text{CO})_9]$ in methanol has four $\nu(\text{CO})$ bands at 2102w (sym. A_1 mode), 2055vs (E), 2039vs (A_1), and 2022w (sh) (E) as expected for a local C_{3v} symmetry.¹⁸ The attachment of a large unsymmetrical group on the carbonyl or by CO replacement by other ligands is known to lead to a splitting of the 2039 cm^{-1} band and the appearance of weaker bands at lower wavenumbers.¹⁸

The SNIFTIRS spectra between -0.6 and -0.9 V of $1.0 \times 10^{-3} \text{ mol dm}^{-3} [\text{Co}_3(\text{CPh})(\text{CO})_9]$ in a CO saturated methanol solution containing $0.1 \text{ mol dm}^{-3} \text{ NaClO}_4$ electrolyte are shown in Fig. 2. All spectra shown were recorded using *p*-polarised light. Spectra were also obtained using *s*-polarised light to test for adsorbed species but no differences were observed between the spectra of the cluster species with different polarisations. The SNIFTIRS spectra recorded between -0.2 (E_s) and -0.6 V during the forward and reverse potential steps showed no absorption changes in the carbonyl region and have been omitted for clarity.

As the electrode potential is stepped from -0.6 to -0.9 V , $[\text{Co}_3(\text{CPh})(\text{CO})_9]$ is reduced to the radical anion $[\text{Co}_3(\text{CPh})(\text{CO})_9]^{-\cdot}$ in the thin solution layer. The negative absorption peaks are due to the loss of $[\text{Co}_3(\text{CPh})(\text{CO})_9]$, whilst the positive absorption peaks at lower wavenumber are due to $[\text{Co}_3(\text{CPh})(\text{CO})_9]^{-\cdot}$. The peaks at 1988 and 1977 cm^{-1} are assigned to the strong E modes of the 49e $[\text{Co}_3(\text{CPh})(\text{CO})_9]^{-\cdot}$, the weaker A_1 mode is seen as a broad ill defined feature at *ca.* 2010 cm^{-1} . For comparison, the $\nu(\text{CO})$ bands of $[\text{Co}_3(\text{CPh})(\text{CO})_9]^{-\cdot}$ occur at 2040w , 1989s , 1973s and 1945vw cm^{-1} in *thf* or CH_2Cl_2 solutions and similar to those of the solid [isolated as its $\text{N}(\text{PPh}_3)_2^+$ salt].⁹ The highest wavenumber weak absorption of $[\text{Co}_3(\text{CPh})(\text{CO})_9]^{-\cdot}$ is not evident due to overlap with other more intense absorptions.

A shift of $60\text{--}70 \text{ cm}^{-1}$ from the 48e to 49e species is compatible with a large increase in charge associated with occupancy of the antibonding a_2 SOMO. This shift is significantly larger than that of 30 cm^{-1} observed when a CO is replaced by a weaker π -acceptor ligand. Of interest is the confirmation from the IR spectra that radical anion formation is reversible in accordance with the CV results shown in Fig. 1(ii). No decomposition products such as $\text{Co}(\text{CO})_4^-$ were observed but there is one weak feature at 1950 cm^{-1} which has not been assigned. This absorption may be due to a dianion but since its intensity correlates with the other $[\text{Co}_3(\text{CPh})(\text{CO})_9]^{-\cdot}$ peaks it is assigned to the E mode of this anion.¹⁸

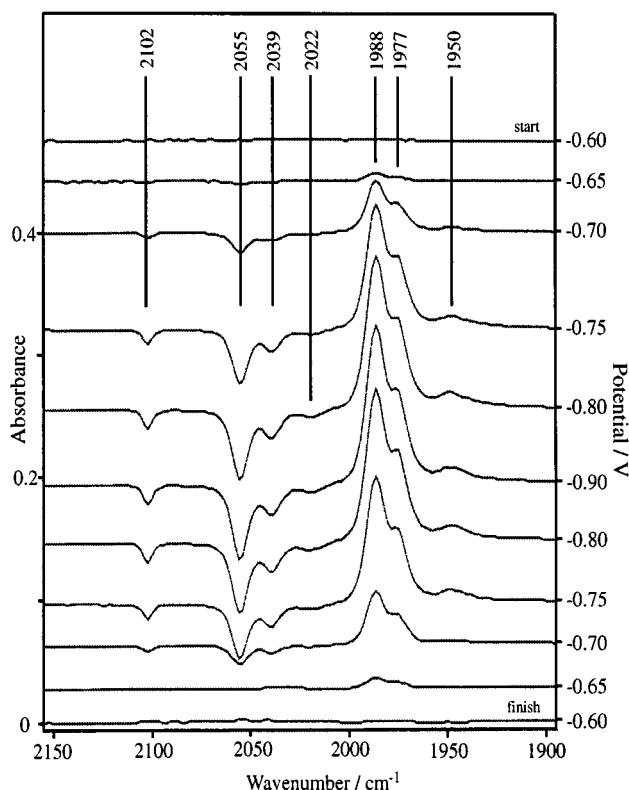


Fig. 2 The SNIFTIRS spectra of $1 \times 10^{-3} \text{ mol dm}^{-3} [\text{Co}_3(\text{CPh})(\text{CO})_9]$ in methanol saturated with CO and containing $0.1 \text{ mol dm}^{-3} \text{ NaClO}_4$ electrolyte. Negative potential steps starting at $E_b = -0.2 \text{ V}$ followed by positive potential steps from -0.9 V

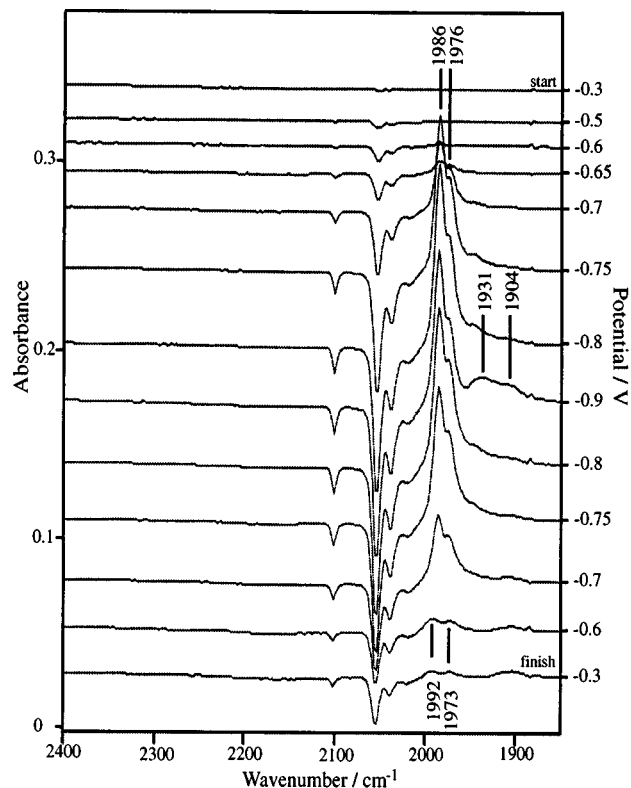


Fig. 4 The SNIFTIRS spectra of $1 \times 10^{-3} \text{ mol dm}^{-3} [\text{Co}_3(\text{CPh})(\text{CO})_9]$ in methanol containing $0.1 \text{ mol dm}^{-3} \text{ NaClO}_4$ electrolyte. Negative potential steps starting at $E_b = -0.2 \text{ V}$ followed by positive potential steps from -0.9 V

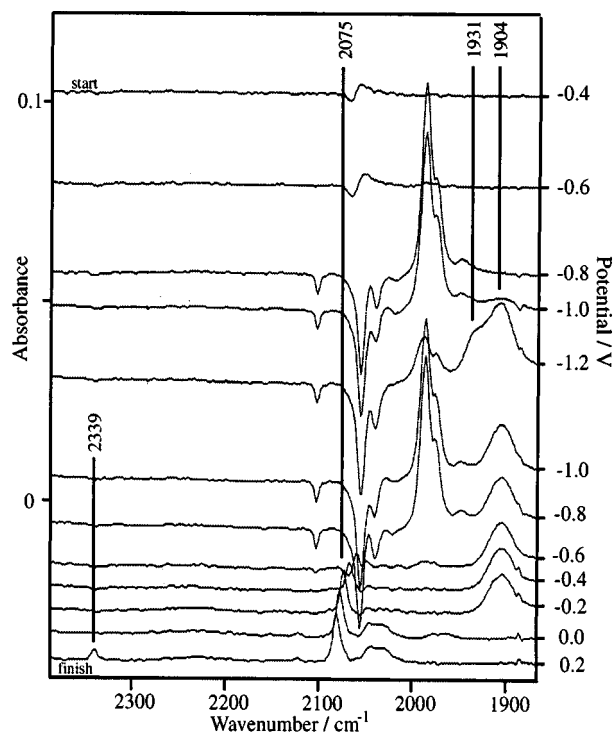


Fig. 3 The SNIFTIRS spectra of $1 \times 10^{-3} \text{ mol dm}^{-3} [\text{Co}_3(\text{CPh})(\text{CO})_9]$ in methanol saturated with CO and containing $0.1 \text{ mol dm}^{-3} \text{ NaClO}_4$ electrolyte. Negative potential steps starting at $E_b = 0.0 \text{ V}$ followed by positive potential steps from -1.2 V

The SNIFTIRS spectra for the extended potential range where the dianion is expected to be observed are shown in Fig. 3. As the electrode potential is stepped from -0.4 to -1.0 V , $[\text{Co}_3(\text{CPh})(\text{CO})_9]$ is reduced to $[\text{Co}_3(\text{CPh})(\text{CO})_9]^{2-}$ as described above. When the potential is stepped further from

-1.0 to -1.2 V there is a decrease in the intensity of the $\nu(\text{CO})$ peaks for $[\text{Co}_3(\text{CPh})(\text{CO})_9]^{2-}$ and at the same time two additional peaks emerge at 1931 and 1904 cm^{-1} . Stepping the potential back to -0.2 V reverses this sequence of events except that the broad feature at 1904 cm^{-1} remains. On this evidence the 1931 cm^{-1} band is assigned to the most intense $\nu(\text{CO})$ E mode of the $50e [\text{Co}_3(\text{CPh})(\text{CO})_9]^{2-}$ species. The shift in energy of *ca.* 60 cm^{-1} is consistent with the addition of a further electron to the a_2 SOMO and is of the order of that encountered for the one-electron reduction of the parent.

The species giving rise to the broad peak at 1904 cm^{-1} remained unoxidised until 0.0 V during the positive potential steps, indicating some irreversible decomposition of the cluster at high negative potentials. In methanol solution $\text{Co}(\text{CO})_4^-$ has a broad band at 1904 cm^{-1} and this assignment was previously confirmed⁹ from the IR spectrum in methanol of the $\text{N}(\text{PPh}_3)_2^+$ salt of this anion. Oxidation of $\text{Co}(\text{CO})_4^-$ during a SNIFTIRS experiment gave a weak and broad absorption centred at *ca.* 2030 cm^{-1} . The most likely candidate for assigning this peak is the most intense E mode of $[\text{Co}_2(\text{CO})_8]$.¹⁹ Absorptions due to solution CO_2 at 2339 cm^{-1} and adsorbed CO at about 2070 cm^{-1} were also present.

A bipolar peak seen at *ca.* 2060 cm^{-1} in Fig. 3 during the initial scan, and the singular peak around 2075 cm^{-1} on the reverse scan, was confirmed by polarisation studies as due to CO adsorbed onto the platinum surface.¹⁴ The peak at 2339 cm^{-1} is due to solution CO_2 .¹⁴ In all of the SNIFTIRS spectra the CO_2 signal emerges as the oxidation of $\text{Co}(\text{CO})_4^-$ is completed. The origin of this CO_2 signal appears to be related to the oxidation of a decomposition product but this remains to be established.

SNIFTIRS spectra of $[\text{Co}_3(\text{CPh})(\text{CO})_9]$ in absolute methanol

The SNIFTIRS spectra between -0.3 and -1.2 V of $1.0 \times 10^{-3} \text{ mol dm}^{-3} [\text{Co}_3(\text{CPh})(\text{CO})_9]$ in absolute methanol are shown in Figs. 4 and 5 (-0.2 to 0.9 V and 0.0 to -1.2 V respectively).

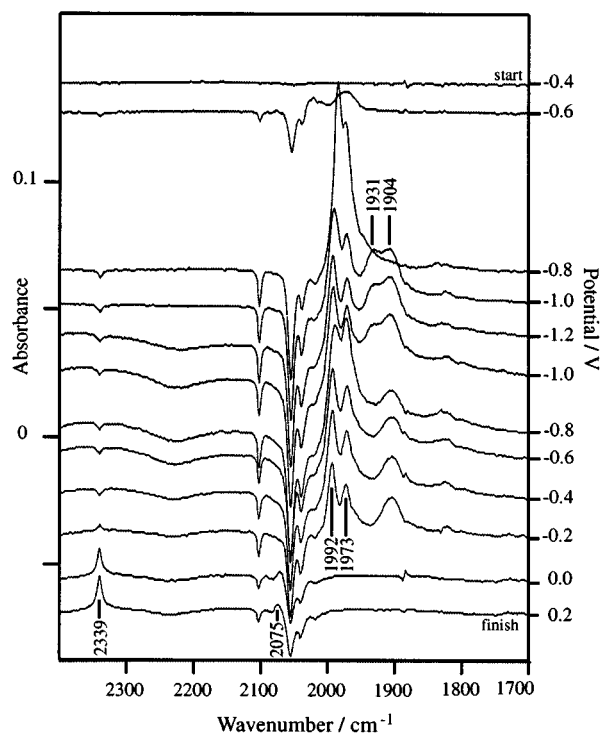


Fig. 5 The SNIFTIRS spectra of $1 \times 10^{-3} \text{ mol dm}^{-3} [\text{Co}_3(\text{CPh})(\text{CO})_9]$ in methanol containing $0.1 \text{ mol dm}^{-3} \text{ NaClO}_4$ electrolyte. Negative potential steps starting at $E_b = 0.0 \text{ V}$ followed by positive potential steps from -1.2 V

These spectra are essentially the same as those in Figs. 2 and 3 from 0.0 V until $E_s = -0.8 \text{ V}$. There was no observable difference between the spectra obtained in either *p*- or *s*-polarised light.

The SNIFTIRS spectra for the reduction of $[\text{Co}_3(\text{CPh})(\text{CO})_9]$ (Fig. 4) produced evidence of cluster decomposition at -0.9 V by the appearance of an infrared peak for $\text{Co}(\text{CO})_4^-$. This is in accordance with the CV results [Fig. 1(i)]. There is also evidence for minor amounts of $[\text{Co}_3(\text{CPh})(\text{CO})_9]^{2-}$ (1931 cm^{-1}) being produced. During the positive potential steps the oxidation of $[\text{Co}_3(\text{CPh})(\text{CO})_9]^-$ to $[\text{Co}_3(\text{CPh})(\text{CO})_9]$ is observed. However, complete recovery of the cluster compound is not achieved when the potential has returned to -0.3 V , with the infrared absorptions of the carbonyl peaks for $[\text{Co}_3(\text{CPh})(\text{CO})_9]$ showing a net loss. This is due to $[\text{Co}_3(\text{CPh})(\text{CO})_9]^-$ decomposition but some diffusion of electroactive material out of the infrared optical path may also contribute.¹⁷ As E_b is approached during the reverse potential steps, two residual peaks at 1992 and 1973 cm^{-1} are observed and will be discussed later in this paper. These peaks are not present in the SNIFTIRS spectra for the CO saturated methanol system (Figs. 2 and 3) and are more clearly observed in Fig. 5 when more negative potentials are applied.

The SNIFTIRS spectra for the extended negative potential region are shown in Fig. 5. These are significantly different at -0.8 V , once reduction of the cluster has begun, from those observed when CO has been added (Fig. 3). There are at least three different species present at -1.0 V . These are $[\text{Co}_3(\text{CPh})(\text{CO})_9]^{2-}$ (1931 cm^{-1}), $\text{Co}(\text{CO})_4^-$ (1904 cm^{-1}) and a species (**Z**) which has two strong absorptions at 1992 and 1973 cm^{-1} . The intensity of the 1904 cm^{-1} band (Figs. 3 and 5) indicates that the majority of the decomposition to $\text{Co}(\text{CO})_4^-$ takes place *via* the $50e$ dianion rather than the $49e$ anion.

To investigate the influence of solvent on the reduction products of the cluster the SNIFTIRS spectra were run in dichloromethane (Fig. 6). Although the bands are not as clearly resolved there is a close correlation with the spectra in methanol solution. The $\nu(\text{CO})$ band wavenumbers of the

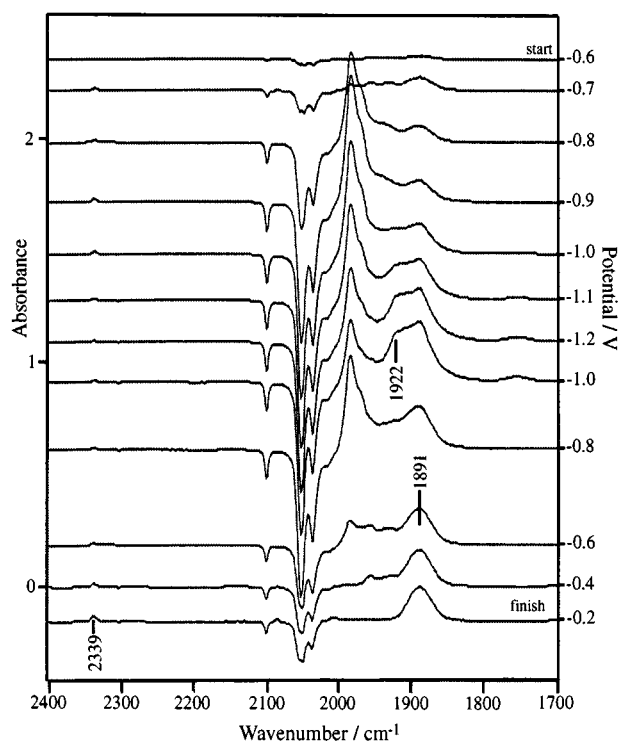


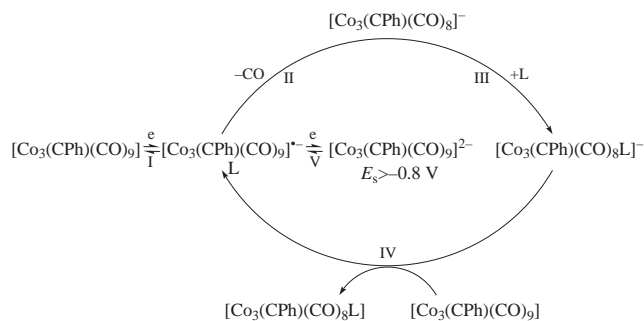
Fig. 6 The SNIFTIRS spectra of $1 \times 10^{-3} \text{ mol dm}^{-3} [\text{Co}_3(\text{CPh})(\text{CO})_9]$ in dichloromethane containing $0.1 \text{ mol dm}^{-3} \text{ NBu}_4\text{ClO}_4$ electrolyte. Negative potential steps starting at $E_b = -0.2 \text{ V}$ followed by positive potential steps from -1.2 V

predominant reduction product, $[\text{Co}_3(\text{CPh})(\text{CO})_9]^-$, are identical. However, there is a marked solvent shift to lower energy of *ca.* 10 cm^{-1} for $\nu(\text{CO})$ of $[\text{Co}_3(\text{CPh})(\text{CO})_9]^{2-}$ and of $\text{Co}(\text{CO})_4^-$. An alternative assignment of the 1922 cm^{-1} band to an octacarbonyl species is unlikely given its behaviour with potential. Such solvent shifts are well known²⁰ for $\text{Co}(\text{CO})_4^-$. What is surprising is the appearance of this decomposition species at -0.7 V before the $49e$ species is observed in the SNIFTIRS spectra. This suggests that another cluster species, unstable in dichloromethane, is being formed at a lower potential.

A clue to this species is provided by a careful examination of Figs. 4 and 5. The two residual peaks at 1992 and 1973 cm^{-1} can be seen in Fig. 4 as E_b is approached during the reverse potential steps. These peaks are not present in the SNIFTIRS spectra for CO saturated methanol solutions (Fig. 2). There is also a change in the intensity profile of the principal product peaks in the potential sequence $-1.2 \rightarrow -0.2 \text{ V}$ in Fig. 5. Species **Z** persists at potentials positive of the $[\text{Co}_3(\text{CPh})(\text{CO})_9]^{0-}$ couple potential.

The wavenumbers of the $\nu(\text{CO})$ peaks for **Z**, as well as the band profile, are similar to those of the $49e$ $[\text{Co}_3(\text{CPh})(\text{CO})_9]^-$ species and suggest that **Z** must be an anion with a closely related structure. The obvious candidate is the $47e$ $[\text{Co}_3(\text{CPh})(\text{CO})_8]^-$ species analogous to the proposed⁷ labile species, $[\text{Co}_3(\text{CMe})(\text{CO})_8]^-$, in the redox cycle of $[\text{Co}_3(\text{CMe})(\text{CO})_9]$.

Oxidation of **Z** led to the decomposition product, $\text{Co}(\text{CO})_4^-$, as is seen in Fig. 5. Clearly, the co-ordinatively saturated $[\text{Co}_3(\text{CPh})(\text{CO})_9]^-$ will be stabilised in the presence of CO and this is observed. Hinkelmann *et al.*⁷ have suggested that this also accounts for the chemical reversibility of the $48e/49e$ couple at high concentrations of $[\text{Co}_3(\text{CR})(\text{CO})_9]$. Electrochemical evidence for the co-ordinatively unsaturated species is inferred from the data obtained from $10^{-5} \text{ mol dm}^{-3}$ solutions. The SNIFTIRS spectra for $5 \times 10^{-5} \text{ mol dm}^{-3} [\text{Co}_3(\text{CPh})(\text{CO})_9]$ in methanol did not allow **Z** and $[\text{Co}_3(\text{CPh})(\text{CO})_9]^-$ to be distinguished.



Scheme 2

SNIFTIRS spectra of $[\text{Co}_3(\text{CPh})(\text{CO})_9]$ in the presence of a phosphine ligand

Phosphines participate in very efficient electron transfer catalysed reactions where the $49e$ $[\text{Co}_3(\text{CPh})(\text{CO})_9]^-$ is the initiating species.² The reduction (or oxidation) of electroactive species in a thin layer arrangement is essentially complete within a very short period of time, of the order of seconds. Therefore a catalytic reaction, once initiated, will proceed quite rapidly, but not necessarily go to completion depending upon the limiting reagent. Scheme 2 is representative of an ETC reaction for $[\text{Co}_3(\text{CPh})(\text{CO})_9]$ and L based upon the scenario put forward by Hinkelmann *et al.*⁷

Fig. 7 contains the SNIFTIRS spectra of $1 \times 10^{-3} \text{ mol dm}^{-3}$ $[\text{Co}_3(\text{CPh})(\text{CO})_9]$ and $1 \times 10^{-3} \text{ mol dm}^{-3}$ $\text{Na}_3[\text{P}(\text{C}_6\text{H}_4\text{SO}_3\text{-}m)_3]$ (L) in methanol with 0.1 mol dm^{-3} NaClO_4 electrolyte. It is clear from the IR spectra that the moment $[\text{Co}_3(\text{CPh})(\text{CO})_9]$ begins to be reduced (at -0.50 V) the substituted cluster, $[\text{Co}_3(\text{CPh})(\text{CO})_8\text{L}]$, is formed. The latter has $\nu(\text{CO})$ peaks at 2078 , 2035 , 2024 and 2013 cm^{-1} . From -0.6 to -0.8 V the IR spectra show a significant amount of $[\text{Co}_3(\text{CPh})(\text{CO})_9]^-$ is present, whilst no further increase in the $\nu(\text{CO})$ peaks for $[\text{Co}_3(\text{CPh})(\text{CO})_8\text{L}]$ is seen. This result is expected as there are two competing pathways in which $[\text{Co}_3(\text{CPh})(\text{CO})_9]$ is being removed (I and IV of Scheme 2). In the thin layer there is a limited supply of $[\text{Co}_3(\text{CPh})(\text{CO})_9]$ and in this case the electrochemical reduction of the cluster dominates. Once $[\text{Co}_3(\text{CPh})(\text{CO})_9]$ has been depleted from the thin layer no further catalysis past step III can occur.

As the potential becomes more negative, the IR spectra predominantly reflect the behaviour that is observed in the absence of L. A notable difference is the increase in the relative intensity of the IR peak (at 1937 cm^{-1}) which has been attributed to $[\text{Co}_3(\text{CPh})(\text{CO})_9]^{2-}$ and the reduction of $[\text{Co}_3(\text{CPh})(\text{CO})_8\text{L}]$. The IR bands for $[\text{Co}_3(\text{CPh})(\text{CO})_8\text{L}]^-$ are expected to be found in much the same wavenumber region as that of $[\text{Co}_3(\text{CPh})(\text{CO})_8]^-$ and this would make identification of these bands difficult. However, $[\text{Co}_3(\text{CPh})(\text{CO})_8\text{L}]^-$ was shown³ to be unstable with respect to decomposition to $[\text{Co}_3(\text{CPh})(\text{CO})_9]$ and, as already observed, reaction II is not significantly competitive. Therefore, the predominant pathway of reduction at $E_s > -0.8 \text{ V}$ is likely to be reaction V. The SNIFTIRS spectra that were run in the presence of a threefold excess of L had a very small peak at *ca.* 1965 cm^{-1} which may be related to $[\text{Co}_3(\text{CPh})(\text{CO})_8\text{L}]^{2-}$.

The IR spectra resulting from the positive potential steps are similar to those observed in solutions without L (or CO). Once $[\text{Co}_3(\text{CPh})(\text{CO})_9]$ has been produced in the thin layer, from the oxidation of $[\text{Co}_3(\text{CPh})(\text{CO})_9]^-$, then the ETC reaction can recommence. At -0.9 V (positive potential steps) the substituted cluster, $[\text{Co}_3(\text{CPh})(\text{CO})_8\text{L}]$, is reformed and is not oxidised further within the potential limits explored here.

Conclusion

The SNIFTIRS results have provided, for the first time, *in situ* infrared spectra of the species produced during the electro-

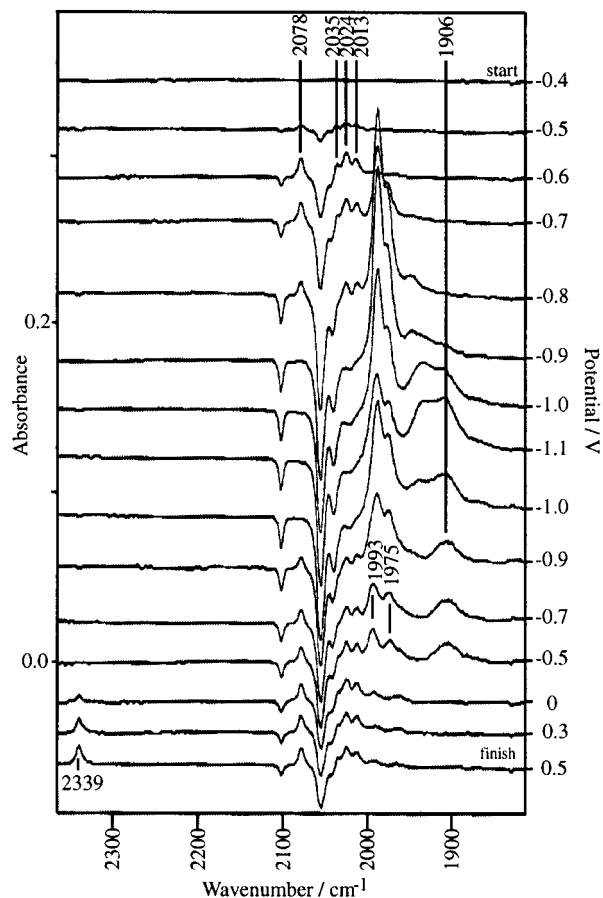


Fig. 7 The SNIFTIRS spectra of $1 \times 10^{-3} \text{ mol dm}^{-3}$ $[\text{Co}_3(\text{CPh})(\text{CO})_9]$ and $1 \times 10^{-3} \text{ mol dm}^{-3}$ $\text{Na}_3[\text{P}(\text{C}_6\text{H}_4\text{SO}_3\text{-}m)_3]$ in methanol containing 0.1 mol dm^{-3} NaClO_4 electrolyte. Negative potential steps starting at $E_b = -0.2 \text{ V}$ followed by positive potential steps from -1.1 V

chemical reduction of $[\text{Co}_3(\text{CPh})(\text{CO})_9]$ in methanol under N_2 , CO and in the presence of a phosphine ligand. From the commonality of electrochemical behaviour for generic $[\text{Co}_3(\text{CR})(\text{CO})_9]$ clusters a similar reaction sequence can be expected for other capped clusters of this type. In general, these results in thin layers concur with the interpretation by Hinkelmann *et al.*⁷ of the solution electrochemistry for $[\text{Co}_3(\text{CMe})(\text{CO})_9]$. There is clear evidence for a co-ordinatively unsaturated species (Z) which is stable over a considerable potential range and the oxidation of which leads to $[\text{Co}_3(\text{CPh})(\text{CO})_9]$. Reduction of $[\text{Co}_3(\text{CPh})(\text{CO})_9]$ gave the species identified as $49e$ $[\text{Co}_3(\text{CPh})(\text{CO})_9]^-$, $50e$ $[\text{Co}_3(\text{CPh})(\text{CO})_9]^{2-}$ and tentatively $47e$ $[\text{Co}_3(\text{CPh})(\text{CO})_8]^-$. The interrelationships between these species at various electrode potentials, and in the presence of CO, were able to be better resolved using the SNIFTIRS technique. Decomposition to $\text{Co}(\text{CO})_4^-$ occurred from both the dianion and the co-ordinatively unsaturated species, but not necessarily from the primary reduction product, $[\text{Co}_3(\text{CPh})(\text{CO})_9]^-$.

The SNIFTIRS spectra for the reduction of $[\text{Co}_3(\text{CPh})(\text{CO})_9]$ in the presence of L clearly show the rapid ETC formation of the neutral product, $[\text{Co}_3(\text{CPh})(\text{CO})_8\text{L}]$. The ETC cycle was quickly suppressed in the thin layer cell due to the depletion of $[\text{Co}_3(\text{CPh})(\text{CO})_9]$. Reduction of the $[\text{Co}_3(\text{CPh})(\text{CO})_8\text{L}]$ species was evident in product IR peaks but the product species was not able to be identified. Since the substituted $[\text{Co}_3(\text{CPh})(\text{CO})_8\text{L}]$ species was able to be identified it should be possible in further studies to investigate the competitive co-ordination that occurs between a chelating and non-chelating phosphine ligand.

Experimental

The compound $[\text{Co}_3(\text{CPh})(\text{CO})_9]$ was prepared by the literature

method and doubly crystallised from hexane.²¹ All manipulations were carried out in an inert atmosphere. Carbon monoxide was used directly from a steel cylinder. As CO from this source has been shown²² to contain [Fe(CO)₅] any iron carbonyl impurity was removed by bubbling the gas through a methanol scrubbing solution containing PPh₃. A comparison of the results obtained during the reduction of [Co₃(CPh)(CO)₉], using CO directly from the steel cylinder or purified as above, showed no observable difference.

Spectroscopy and electrochemistry

Measurements were made at 20 °C with purified solvents. Acetone was removed from the reagent-grade methanol by fractional distillation from iodoform and dried by fraction distillation from Mg/I₂ then standing over activated 4 Å molecular sieves. The water content was less than 0.01 vol. % (typically between 0.008 and 0.003 vol. %) water as determined by the Karl Fischer titration using a biampometric end-point detection method.²³ Dichloromethane was washed with aqueous alkali, distilled, dried over activated 4 Å molecular sieves²⁴ and stored in the dark under nitrogen. Electrolyte solutions were freshly prepared prior to each experiment from anhydrous NaClO₄ or tetrabutylammonium perchlorate.

All potentials are with respect to an aqueous KCl saturated calomel electrode (SCE). Electrode potential control, electrochemical data and SNIFTIRS were obtained using an EG & G Princeton Applied model 363 potentiostat coupled to a HB Thompson & Associates model DRG16 ramp generator for cyclic voltammetry. Working potentials were monitored with a Thandar TM351 digital multimeter and the *I/A* vs. *E/V* plots recorded on a Houston X-Y recorder.

Cyclic voltammograms were conducted in a standard three electrode cell comprising platinum disc working and platinum wire secondary electrodes with an aqueous KCl saturated calomel electrode. Solutions were purged with oxygen-free nitrogen before measurements. The polished platinum working electrode and other components of the electrochemical cell were similar to those previously described.¹⁴ The platinum working electrodes were polished with 0.015 µm Al₂O₃ before being subjected to an electrochemical cleaning treatment which consisted of 30 s of potential stepping between 4.0 and -4.0 V at 2 Hz in 0.5 mol dm⁻³ aqueous H₂SO₄ solution. Such a treatment gave well resolved adsorbed hydrogen peaks in a cyclic voltammogram recorded in the 0.5 mol dm⁻³ H₂SO₄ solution. The electrode was then successively rinsed with water, methanol and a portion of the cell solution before being placed in the spectroelectrochemical cell without allowing the electrode surface to dry at any stage of the rinsing.

The infrared spectra were obtained with a Digilab FTS60V evacuable optical bench spectrometer equipped with a mercury cadmium telluride detector and coupled to a thin layer electrochemical cell *via* a CaF₂ 60° dove prism. A description of the SNIFTIRS cell and evacuable optical bench will be given elsewhere.¹² The SNIFTIRS spectra were obtained with a solution layer of about 5 µm between the electrode and the CaF₂ prism. The lower limit of the wavenumber range was determined by the CaF₂ absorption. All spectra were recorded at 4 cm⁻¹ resolution with an acquisition time of 60 s at each potential after 30 s was allowed for steady state conditions to be achieved. The noise level over most of the spectral range was less than 0.0002 absorbance.

Acknowledgements

We thank the Research Committee of the University of Otago

for financial support. P. A. B. acknowledges Ph.D. funding from the University of Otago.

References

- 1 N. G. Connelly and W. Geiger, *Adv. Organomet. Chem.*, 1985, **24**, 87.
- 2 B. H. Robinson and J. Simpson, *Paramagnetic Organometallic Species in Activation/Selectivity Catalysis*, ed. M. Chanon, Kluwer, Dordrecht, 1989, p. 357.
- 3 C. M. Arewgoda, B. H. Robinson and J. Simpson, *J. Chem. Soc., Chem. Commun.*, 1982, 284; G. J. Bezems, P. H. Rieger and S. J. Visco, *J. Chem. Soc., Chem. Commun.*, 1981, 265; C. M. Arewgoda, B. H. Robinson and J. Simpson, *J. Am. Chem. Soc.*, 1983, **105**, 1893; A. J. Downard, B. H. Robinson and J. Simpson, *Organometallics*, 1986, **5**, 1122.
- 4 M. I. Bruce, D. C. Kehoe, J. G. Matison, B. K. Nicholson, P. H. Rieger and M. L. Williams, *J. Chem. Soc., Chem. Commun.*, 1982, 442; A. Dachen, C. Mahe and H. Patin, *J. Chem. Soc., Chem. Commun.*, 1982, 243; R. G. Cunninghame, A. J. Downard, L. R. Hanton, S. D. Jensen, B. H. Robinson and J. Simpson, *Organometallics*, 1984, **3**, 180; R. G. Cunninghame, L. R. Hanton, S. D. Jensen, B. H. Robinson and J. Simpson, *Organometallics*, 1987, **6**, 1470; S. D. Jensen, B. H. Robinson and J. Simpson, *Organometallics*, 1987, **6**, 1479.
- 5 B. M. Peake, B. H. Robinson, J. Simpson and D. J. Watson, *Inorg. Chem.*, 1977, **16**, 410; A. M. Bond, U. Honrath, P. N. T. Lindsay, B. M. Peake, B. H. Robinson, J. Simpson and H. Vahrenkamp, *Organometallics*, 1984, **3**, 413; A. J. Downard, B. H. Robinson and J. Simpson, *Organometallics*, 1986, **5**, 1132.
- 6 A. M. Bond, B. M. Peake, B. H. Robinson, J. Simpson and D. J. Watson, *Inorg. Chem.*, 1977, **16**, 2199.
- 7 K. Hinkelmann, J. Heinze, H.-T. Schacht, J. S. Field and H. Vahrenkamp, *J. Am. Chem. Soc.*, 1989, **111**, 5078.
- 8 B. M. Peake, P. H. Rieger, B. H. Robinson and J. Simpson, *Inorg. Chem.*, 1979, **18**, 1000; 1981, **20**, 2540; S. B. Colbran, L. R. Hanton, B. H. Robinson, W. T. Robinson and J. Simpson, *J. Organomet. Chem.*, 1987, **330**, 415.
- 9 P. N. T. Lindsay, Ph.D. Thesis, University of Otago, 1982.
- 10 N. W. Duffy, B. H. Robinson, K. Robinson and J. Simpson, *J. Chem. Soc., Dalton Trans.*, 1994, 2821.
- 11 M.-C. Pham, F. Adami, P.-C. Lacaye, J.-P. Doucet and J.-E. Dubois, *J. Electroanal. Chem. Interfacial Electrochem.*, 1986, **201**, 413.
- 12 J. G. Love, P. A. Brooksby and A. J. McQuillan, unpublished work.
- 13 P. A. Brooksby, C. A. Hunter, A. J. McQuillan, D. H. Purvis, A. E. Rowan, R. J. Shannon and R. Walsh, *Angew. Chem., Int. Ed. Engl.*, 1994, **33**, 2489; A. Babaei and A. J. McQuillan, *J. Phys. Chem.*, 1997, **101**, 7443.
- 14 J. G. Love and A. J. McQuillan, *J. Electroanal. Chem. Interfacial Electrochem.*, 1989, **274**, 263.
- 15 R. H. Wopschall and I. Shain, *Anal. Chem.*, 1967, **39**, 1514.
- 16 A. J. Bard and L. R. Faulkner, *Electrochemical Methods*, Wiley, New York, 1980.
- 17 *Spectroelectrochemistry: Theory and Practice*, ed. R. J. Gale, Plenum, New York, 1988; K. Ashley and S. Pons, *Chem. Rev.*, 1988, **88**, 673; T. Iwasita and F. C. Nart, *Adv. Electrochem. Sci. Eng.*, 1995, **4**, 126.
- 18 G. Bor, *Proc. Symp. Coord. Chem. Tihany*, 1964, 361.
- 19 P. S. Braterman, *Metal Carbonyl Spectra*, Academic Press, London, 1975.
- 20 W. F. Edgell and S. Chanjamai, *J. Am. Chem. Soc.*, 1980, **102**, 147 and refs. therein.
- 21 W. T. Dent, L. A. Duncanson, R. G. Guy, H. W. B. Reed and B. L. Shaw, *Proc. Chem. Soc.*, 1961, 169.
- 22 A. Cuesta and C. Gutierrez, *J. Electroanal. Chem. Interfacial Electrochem.*, 1995, **395**, 331.
- 23 *Standard Test Method for Water in Volatile Solvents (Fischer Reagent Titration Method)*, The American Society for Testing and Materials, Annual Book of ASTM Standards, 1982, Part 29, D1364-78, pp. 175-178.
- 24 A. Weissberger, in *Techniques in Chemistry*, eds. J. A. Riddick and W. B. Bunger, Wiley, New York, 3rd edn., 1970, vol. 2.

Received 13th May 1998; Paper 8/03596B